ACS APPLIED MATERIALS & INTERFACES

Research Article

www.acsami.org

Implementation of High-Quality Warm-White Light-Emitting Diodes by a Model-Experimental Feedback Approach Using Quantum Dot–Salt Mixed Crystals

Marcus Adam,[†,⊥] Talha Erdem,[‡,⊥] Gordon M. Stachowski,[†] Zeliha Soran-Erdem,[‡] Josephine F. L. Lox,[†] Christoph Bauer,[†] Jan Poppe,[†] Hilmi Volkan Demir,[*,‡,§] Nikolai Gaponik,[*,†] and Alexander Eychmüller[†]

[†]Physical Chemistry, TU Dresden, Bergstr. 66b, 01062 Dresden, Germany

[‡]Department of Electrical and Electronics Engineering, Department of Physics, and UNAM-Institute of Materials Science and Nanotechnology, Bilkent University, TR-06800 Ankara, Turkey

[§]LUMINOUS! Center of Excellence for Semiconductor Lighting and Displays, School of Electrical and Electronic Engineering and School of Physical and Mathematical Sciences, Nanyang Technological University, Singapore 639798, Singapore

Supporting Information

ABSTRACT: In this work, a model-experimental feedback approach is developed and applied to fabricate high-quality, warm-white light-emitting diodes based on quantum dots (QDs) as color-conversion materials. Owing to their unique chemical and physical properties, QDs offer huge potential for lighting applications. Nevertheless, both emission stability and processability of the QDs are limited upon usage from solution. Incorporating them into a solid ionic matrix overcomes both of these drawbacks, while preserving the initial optical properties. Here borax ($Na_2B_4O_7{\cdot}10H_2O$) is used as a host matrix because of its lower solubility and thereby reduced ionic strength in water in comparison with NaCl. This guarantees the stability of high-quality CdSe/ZnS QDs in the aqueous phase during crystallization and results in a 3.4 times higher loading amount of QDs within the borax crystals compared to NaCl. All steps from the synthesis via mixed crystal preparation to the warm-white LED preparation are verified by applying the model-experimental feedback, in which experimental data and numerical results provide feedback to each other recursively. These measures are taken to ensure a high luminous efficacy of optical radiation (LER) and a high color rendering index (CRI) of the final device as well as a correlated color temperature (CCT) comparable to an incandescent bulb. By doing so, a warm-white LED with a LER of 341 lm/W_{opt}, a CCT of 2720 K and a CRI of 91.1 is produced. Finally, we show that the emission stability of the QDs within the borax crystals on LEDs driven at high currents is significantly improved. These findings indicate that the proposed warm-white light-emitting diodes based on QDs-in-borax hold great promise for quality lighting.

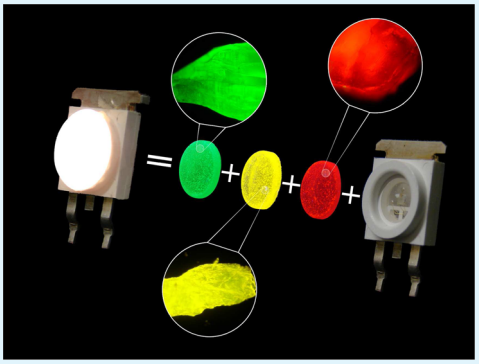

KEYWORDS: *white LEDs, color conversion, mixed crystals, quantum dots, composites, colloidal nanocrystals*

INTRODUCTION

Throughout history, light has been an essential necessity for all types of life and therefore also a central point of culture and science.[1] Two hundred years after Augustin-Jean Fresnel's theory of light as a wave, 2015 is the UNESCO's "International Year of Light and Light-based Technologies".[2] Therefore, broad attention will be placed on all of its application areas, while we still use one-fifth of our end-point electricity powering luminaires.[3] With this, lighting is a major component of energy consumption and offers the possibility for major savings to reach worldwide goals for reducing the energy demand. To decrease the electricity consumption, Edison's incandescent bulb was recently banned from the European markets due to its low efficiency.[4] At the same time, energy saving fluorescent lamps being the first-generation replacements of their incandescent counterparts raise concerns about their safety due to their mercury content, which is only barely encapsulated. Solid state lighting (SSL) technologies, which were essentially initiated by the development of the first blue light-emitting diodes (LEDs)[5] and recently awarded with a Nobel Prize in physics, step forward to fill the still vacant position of next-generation, high-quality indoor luminaires. Today's commercially available white LEDs (w-LEDs) mainly suffer from the trade-off between the color rendering index (CRI) and the luminous efficacy of optical radiation (LER) due to their broadband-emitting color converting phosphors. These are based on rare-earth doped oxides with a long emission tail reaching the deep-red part of the spectrum where the eye is not

Received: September 7, 2015
Accepted: October 6, 2015
Published: October 6, 2015

DOI: 10.1021/acsami.5b08377
ACS Appl. Mater. Interfaces 2015, 7, 23364–23371

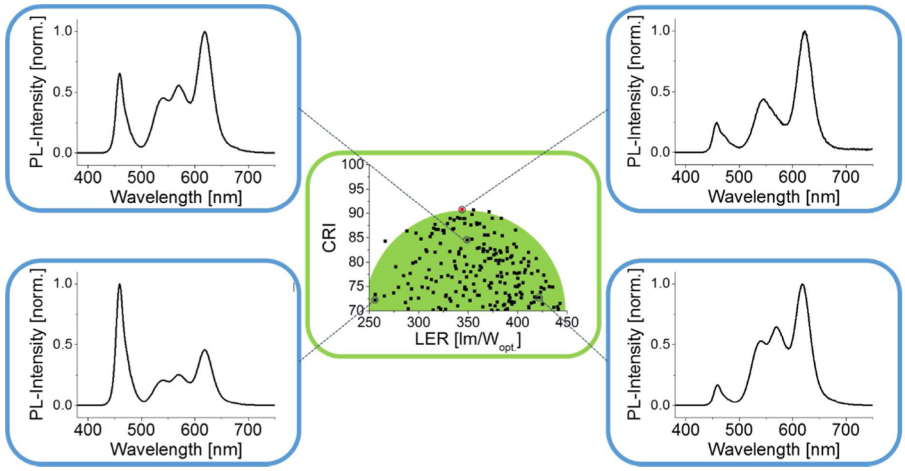

Figure 1. Overview of feasible CRI-LER combinations (black squares) with the experimentally prepared mixed crystals used as color conversion materials on blue LEDs (center). The two PL-spectra on the left and the bottom right one show theoretically determined combinations corresponding to the marked points on the CRI-LER plane. The top right PL-spectra and the corresponding red square show the photometric performance of the most optimized final w-LED.

sensitive while not providing a sufficient amount of red photons in the visible region.[6,7] One solution to overcome this issue is the use of fluorescent colloidal semiconductor quantum dots (QDs) as color converters. Discovered in the 1980s,[8,9] QDs own altered chemical and physical properties compared to their bulk counterparts and provide the band gap tunability with their size enabled by size-dependent quantum confinement effects.[10] Therefore, emitters with a tunable emission peak accompanied by a narrow full-width-at-half-maximum (fwhm) spanning a significant portion of the electromagnetic spectrum can be obtained using the same material system.[11] Their application as color converters on LEDs[12−17] has been successfully demonstrated; however, their limited stability against oxidation and decomposition remains a challenge to overcome. In our previous publication,[18] we addressed this problem by incorporating the QDs into ionic matrices, e.g., NaCl and KCl and drastically improved their photostability while preserving or, under the right conditions, increasing their photoluminescence quantum yield (PL-QY).[19]

Although these QD−salt mixed crystals proved to be suitable as color conversion materials,[18,20−24] only proof-of-concept w-LEDs without any photometric optimization were shown. In this study, we carried out a model-experimental feedback approach to prepare QD−salt mixed crystals, which can be used to produce w-LEDs with a high LER, a high CRI and a low correlated color temperature (CCT) comparable to the incandescent bulb. First, we used the model to identify the spectral requirements for high-quality lighting employing QD photoluminescence (PL) spectra, which were then implemented in the subsequent QD synthesis. By comparing the experimental spectra at each intermediate stage with the model, we optimized the color quality and photometric efficiency of the final w-LED. In addition, here we benefitted for the first time from the reduced ionic strength of borax in water compared to NaCl allowing significantly higher loading of QDs into crystals making the implementation of the designed w-LEDs possible. Finally, we showed that the encapsulation of the QDs in salt crystals provides outstanding emission stability integrated with LEDs driven at high currents.

RESULTS AND DISCUSSION

Modeling. We used the photometric calculations as the feedback tool for the design of our white LEDs. The first step of our work has been the determination of the number of color components. According to Tsao,[25] four color components, i.e., blue, green, yellow, and red, are required for achieving high-quality white light. In our previous work, we determined the required wavelengths, relative amplitudes, and full-width-at-half-maximum values of the QD emitters.[26] In light of this prior work, here we chose to use a blue LED emitting at 460 nm, green-emitting QDs with the peak emission around 530−540 nm, and red-emitting QDs with the peak emission around 620 nm. Although the necessary condition for the yellow peak wavelength to achieve high-quality lighting was found to be 570−580 nm, we chose to use the yellow component to fine-tune the white LED spectrum as the experimental implementation slightly differs from the theoretical calculations. For this purpose, we prepared green and red QD mixed crystals and recorded their PL spectra before preparing the yellow QD mixed crystals. Our calculations showed that employing the blue LED together with these green and red mixed crystals cannot provide high LER and high CRI together with warm-white shade at the same time, confirming the results of ref 25. Furthermore, to determine the conditions for high-quality white light, we calculated the required peak emission wavelength of the yellow color component by making use of the PL-spectra of the green and red mixed crystals along with that of the blue LED. Because the material composition and the synthesis methodology of the yellow QDs are similar to those of the green QDs, we selected the fwhm values of the yellow QDs to be the same as that of the green QDs. Our calculations revealed that the peak emission wavelength around 570 nm allows for realizing CRI > 90, LER ∼ 350 lm/W$_{opt}$, and CCT < 3000 K, all at the same time. On the basis of this information, yellow mixed crystals emitting at 573 nm were grown. In the center of Figure 1, possible CRI-LER combinations of the modeled LEDs based on experimentally prepared mixed crystals are shown as black squares, whereas the green background is a guide for the eye showing feasible combinations. The PL-spectrum display exemplarily chosen possible combinations of the four colors and their correspond-

DOI: 10.1021/acsami.5b08377
ACS Appl. Mater. Interfaces 2015, 7, 23364−23371

ing photometric performance. Subsequently, the required relative amplitudes of the integrated PL-intensities of the respective color components were determined using the experimental emission spectra of the QD-salt crystals and the blue LED to be 2/9 for both the blue and green components, 1/9 for the yellow component, and 4/9 for the red color component to achieve high color quality and photometric performance. On the basis of these calculations, a white LED made of these mixed crystals was prepared simultaneously experimentally achieving CRI = 91, LER = 341 lm/W_{opt}, and CCT = 2720 K, marked as a red square in the center and the corresponding PL-spectra shown in the upper right corner of Figure 1.

QD Synthesis. Oil-based CdSe/ZnS QDs with an alloyed gradient shell were used, because they show a better tunability in the higher photon energy part of the spectrum and a narrower fwhm in the lower energy region compared to aqueous-based CdTe QDs while preserving high stability and PL-QY. In Figure 2, the PL-spectra of the resulting QDs are

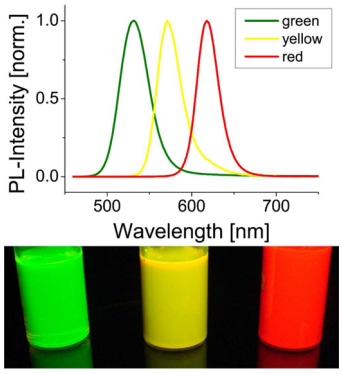

Figure 2. PL-spectra (top) and true color images under UV-excitation at 365 nm (bottom) of three different CdSe/ZnS QDs samples. The QDs are dispersed in $CHCl_3$ and stored under ambient conditions.

shown, with emission maxima at 530, 570, and 617 nm, fwhm values of 40, 30, and 30 nm and PL-QY values 38.5%, 40.2%, and 42.6% for green, yellow and red, respectively. These fwhm values are in agreement with the requirements of high-quality lighting as described in ref 26. Below the PL-spectra in Figure 2, a photograph of the QD solutions under UV excitation shows their bright, pure color emission. Because Cd-based materials possess an inherent toxicity, their usage in general applications is highly restricted. Nevertheless, if the benefits of using Cd-based materials strongly exceeds the risks, their application can be permitted by the legislature, as some current attempts indicate for the use of Cd-based QDs in display color enrichment and general lighting color conversion applications within the European Union.[27]

Ligand Exchange. The used oil-based QDs are stabilized by OA and TOP and are not soluble in the saturated, aqueous borax solution. Therefore, a phase transfer together with a ligand exchange toward the short chain thiol MPA is necessary. As it can be seen from Figure 3, QDs are transferred toward the initially colorless aqueous phase, preserving their pure color and intense emission (Figure 3d). The transfer is quantitative, yielding a colorless $CHCl_3$ phase and no aggregated particles, proving well stabilized, ligand exchanged QDs. Both shape and position of the PL-spectra stay constant during the procedure, as can be seen in Figure S1. During the ligand exchange,

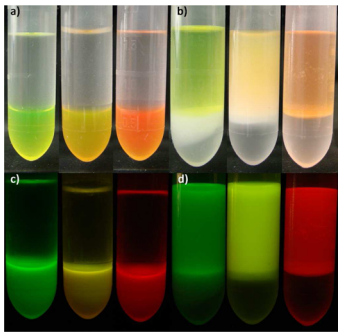

Figure 3. True color images of three different CdSe/ZnS QDs before (a and c) and after (b and d) ligand exchange under ambient light (top) and 365 nm UV-excitation (bottom).

nonideal surface passivation is achieved, which causes a typical decrease of the PL-QY to roughly 50% of the initial value.[28,29]

Mixed Crystal Preparation. Embedding the ligand exchanged QDs into NaCl is known to be nontrivial, because their stability, in comparison to initially aqueous-based CdTe QDs is lower.[19] Using NaCl as a host, only mixed crystals with small loading amounts of QDs can be obtained, as is shown in Figure S2. To overcome these problems, either different crystallization procedures like the liquid−liquid diffusion assisted crystallization (LLDC)[24] or controlled co-precipitation methods[30,31] can be used. However, the LLDC delivers QD loadings that are still insufficient for the highest-quality color conversion.[24] At the same time, coprecipitation methods typically utilize thiol-capped CdTe QDs.[30,31] These limitations can be avoided if borax is used as the host material. Owing to its much lower solubility in water in comparison to NaCl (0.13 mol/L compared to 6.14 mol/L, respectively),[32] the ionic strength of the saturated borax solution is much lower than that of the saturated NaCl solutions. Therefore, the stability of the ligand exchanged QDs is much higher within the borax solution. That is why using the same amount of QDs per mL of the saturated salt solution should result in a higher QD loading within the borax. Stripping voltammetry measurements (Table S2) showed a 3.4 times higher amount of Cd within the borax- in comparison to the NaCl-based mixed crystals prepared from the same batch of ligand exchanged QDs. Thus, we can conclude that, as expected, the loading of the QDs is also 3.4 times higher in the case of borax. In Figure 4, the resulting borax based mixed crystals are displayed. As can be seen from the microscopic images in Figure 4b,e,h, the QDs are reasonably uniformly distributed within the matrix. The corresponding PL-spectra show that upon incorporation the pure color emission does not change, but a small red shift of the emission maxima occurs. This small shift can be caused by the change of the dielectric constant and the refractive index when transferring the particles from water to the salt matrix.[18,19] The PL-spectrum in Figure 4f show a reproducible slight red tailing, indicating a small amount of aggregated QDs upon incorporation into borax. Such slight broadening, in the case of the yellow component, does not reduce the overall quality of the color converter in a significant way. To ensure that the spectral properties of the mixed crystals will not change upon milling and incorporation into the silicone, thin layers of powder encapsulated into the silicone resin were prepared. The corresponding spectra can be found in Figure S3, showing no change during the silicone embedding process. For all samples, PL-LT and PL-QY measurements were conducted in $CHCl_3$,

DOI: 10.1021/acsami.5b08377
ACS Appl. Mater. Interfaces 2015, 7, 23364−23371

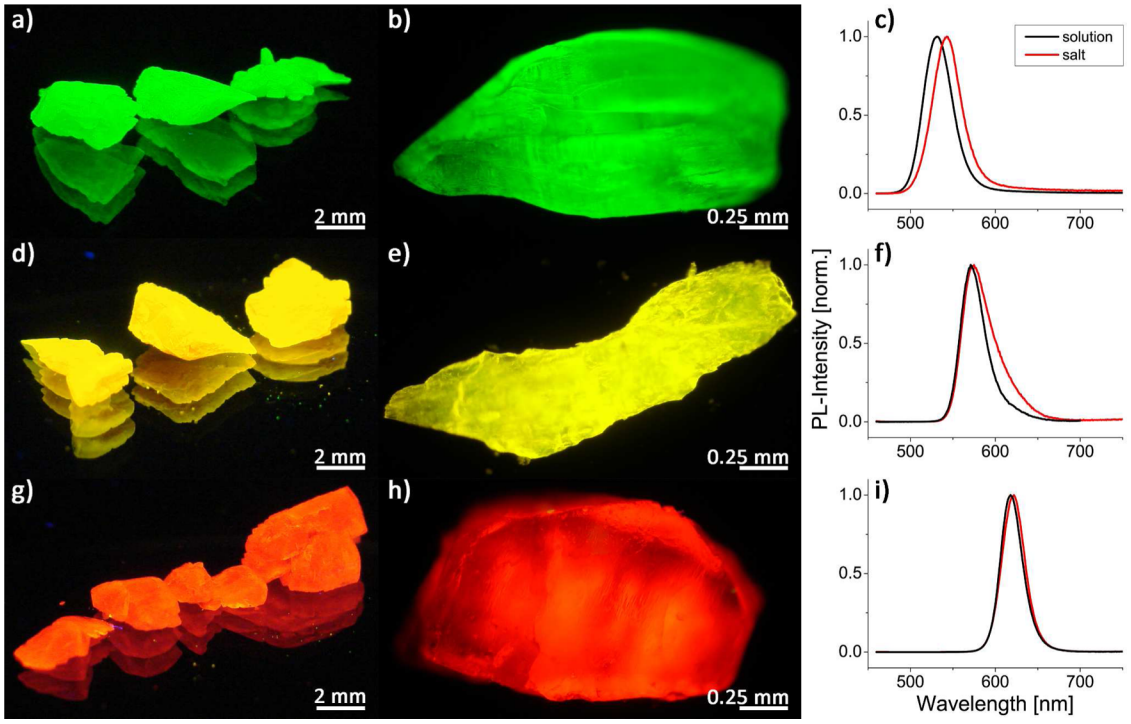

Figure 4. True color (a, d, and g) and microscopic (b, e, and h) images of differently emitting CdSe/ZnS QDs incorporated into borax crystals under UV-excitation (365 nm). Panels c, f, and i show the corresponding PL-spectra of the initial solutions (black lines) and mixed crystals (red lines).

H_2O, and borax, the corresponding results are given in Figure S4 and Table S3. As expected from the recent studies on mixed crystals,[19,20,24] all samples show a stronger change in the PL-QY than PL-LT over all steps (and thereby during changing the surrounding media), whereas both figures exhibit similar trends. Such behavior was previously discussed in the literature,[33] considering the fact that both PL-QY and PL-LT data arise from ensemble measurements of QDs revealing multiexponential decay kinetics. In such ensembles, PL-LT measurements are commonly dominated by the strongest luminescent component, whereas PL-QY measurements account also for weakly emitting (or dark) QDs due to their absorbance and reflect most likely a broad distribution in PL-QY. Therefore, to date, no straightforward correlation between the QDs PL-QY and PL-LT has been found, as it is, on the other hand, well-known for molecular emitters.[34] Second, the results are in good agreement with the findings of our recent mixed crystal PL-QY study.[19] An encapsulation of CdSe/ZnS QDs into an ionic matrix does not lead to a pronounced increase in PL-QY, because no passivating $CdCl_x$ can be formed on the QDs surface.

To verify that the QDs are well dispersed within the borax matrix, the mixed crystals were embedded within a resin and cut into thin sheets using an ultramicrotome. This step proved to be necessary, because directly adding the mixed crystals (or powders thereof) on top of the TEM-grid resulted in fast and complete melting of the mixed crystals under electron beam exposure.[18] The images in Figure 5 show reasonably well-separated and nonaggregated QDs within the salt matrix, which is in good agreement with the results from the optical characterization methods. It should be highlighted that only using these thin sheets, imaging of the QDs within an inorganic crystal matrix at atomic resolution, showing the crystallographic planes of the QDs is possible. Although a similar approach was used for QDs within NaCl-based mixed crystals,[24] only borax

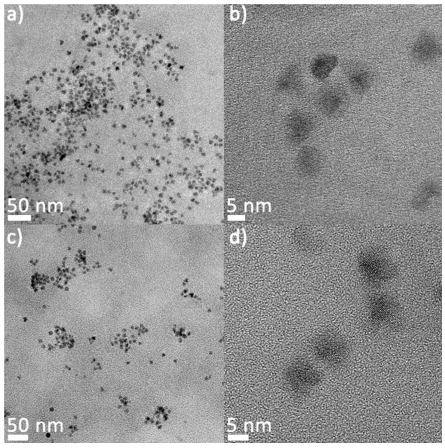

Figure 5. TEM images of the green (a and b) and red (c and d) emitting mixed crystals shown in Figure 4. Overviews (a and c) as well as highly magnified images (b and d) of the samples prove nonaggregated and well distributed QDs within the matrix.

proved to be suitable as a stable matrix under electron beam exposure, allowing for such high magnifications.

Stability Tests of the White LED. The emission intensity of the QD mixed crystals was recorded by hybridizing them on a blue LED driven at 300 mA for 96 h (4 days). To avoid a pronounced heat generation, the LED was placed on an aluminum plate for passive cooling and operated with a 1 kHz on/off rate. Under these conditions, the LED's temperature stayed below 35 °C (see Figure S5) whereas a continuous operation did cause an increase to 72 °C, which would reduce the overall stability of the emissive layer. Figure 6 displays the PL-spectra recorded during the investigation. The intensity of the mixed crystal emission only slightly decreases, which is in good agreement with our recent findings on the PL-stability of

DOI: 10.1021/acsami.5b08377
ACS Appl. Mater. Interfaces 2015, 7, 23364−23371

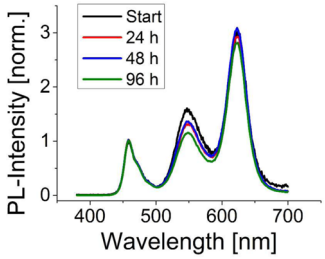

Figure 6. PL-spectra of the w-LED before and during the stability tests. The w-LED was driven at 300 mA and a 1 kHz on/off rate, avoiding significant heat generation.

the mixed crystals under intense illumination.[18] Therefore, these mixed crystals outcompete most of other QD packaging approaches in terms of photostability, verifying their suitability in color conversion applications. It should be noted that the mixed crystals were grown under ambient conditions. For commercialization, a preparation under inert atmosphere could be beneficial, preventing the incorporation of dissolved O_2 and might be a crucial step to increase further the overall photostability.

W-LED Preparation. To produce our final w-LED, the described mixed crystals were milled to a fine powder and dried. Defined amounts of green (20 mg), yellow (8 mg), and red (16 mg) mixed crystal converters were blended together with a two-component, industrial standard silicone resin. The given mass amounts do not strictly correlate with the calculated relative PL-intensities due to the variations in QD loadings and different PL-QY values of the conversion materials.

During initial preparations, a swelling of the powder−silicone mixture was observed, causing an inhomogeneous and porous conversion layer, as shown in Figure 7b. These layers showed

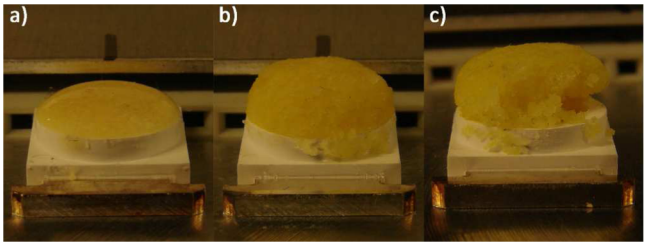

Figure 7. True color image of a LED (a) prepared using borax powder that was dried before blending it with the silicone on top of the LED. Photographs in panels b and c show LEDs produced using nondried mixed crystal powder. Panel b shows the porous and nonhomogenous silicone encapsulation, and panel c displays the minor mechanical stability of such layers.

low mechanical stability (Figure 7c, conversion layer after holding with tweezers) and provided only weak protection of the fine powder against oxygen and water-vapor diffusion, yielding a change of the w-LEDs spectra within days. Borax, unlike our recently used matrices NaCl, KCl, etc., crystallizes as a decahydrate. As it can be seen from the thermogravimetric analyses of the borax-based mixed crystals in Figure S6, parts of the crystal water are released at 70 °C, the curing temperature of the silicone. Gently drying the mixed crystal powder under vacuum at 70 °C before blending it with the silicone ensures that no further crystal water is released during curing, yielding a smooth and rigid conversion layer as shown in Figure 7a. Removing parts of the crystal water during the drying step also reduces the overall mass of mixed crystal powder needed, enabling the formation of smaller conversion layers. Moreover, upon removing the crystal water the PL-QY stays constant within measurement uncertainties.

By adjusting the amounts of green, red, and yellow powder, the hue of the final device can be tuned to a warm white. Figure 8d shows the emission spectrum of the resulting warm-white LED achieving a CCT of 2720 K, a CRI of 91 and a LER of 341 lm/W_{opt} simultaneously. These values combine a warm-white hue, which is comparable to an incandescent bulb (CCT ∼ 2800 K), while preserving the high efficiency of the SSL-devices and giving a color rendering, which matches industrial requirements.[35] Furthermore, it overcomes the CRI = 90 barrier of QD-based LEDs for the first time simultaneously reaching LER > 340 lm/W_{opt} with a warm-white shade, exceeding the current state-of-the art in the literature.[36] Several studies presented promising w-LEDs with QD-based conversion layers and a CRI close to and above 90, using either Cd-containing[36,37] or Cd-free[15,38,39] QDs. Nevertheless, none of them managed to reach simultaneously a CRI > 91 while providing a CCT < 3000 K as well as a LER > 340 lm/W_{opt}, thereby balancing these strongly related figures of merit.

In Figure 8e, the position of the LEDs spectra within the CIE 1931 diagram (x = 0.4557, y = 0.4056) and a blackbody radiator are marked with the cross and the black curve, respectively. Figure 8a shows the QD−salt mixed crystals that we used to produce our w-LED under the illumination of a standard fluorescence lamp. In comparison, the same image was taken in the darkened room, just illuminated by our w-LED (Figure 8b). Here, especially the red crystals show a more saturated color in comparison to Figure 8a, which is due to the LEDs much higher amount of emitted red light in comparison to the fluorescent lamp. Because most of today's commercially available w-LEDs also lack a sufficient amount of red within their emission spectra, the fluorescent lamp can be used as a comparison. Figure 8c shows the same image taken under 365 nm UV-excitation, proving the intense and pure color emission of the mixed crystals.

CONCLUSION

In summary, we presented a model-experimental feedback approach to prepare CdSe/ZnS QDs with an alloyed gradient shell whose emission spectra match the requirements of high-quality white-light luminaires. These QDs were successfully phase-transferred and incorporated in borax-based mixed crystals, which provide a rigid and airtight ionic matrix while assuring a high loading density of the QDs. For the stability test, these mixed crystals showed an exceptional high stability, proving their applicability as color converters. Throughout all steps, intermediate results were reviewed with the spectral model to ensure their applicability as color conversion materials. Finally, by hybridizing green-, yellow-, and red-emitting mixed crystals onto a blue LED, we demonstrated a white LED with a correlated color temperature of 2720 K, a color rendering index of 91.1, and a luminous efficacy of optical radiation of 341 lm/W_{opt}.

EXPERIMENTAL SECTION

Model for Spectral Evaluation. To maximize the photometric performance of the w-LEDs, we carefully designed the spectra of the LEDs prior to experiments so that fitting QDs could be used with the correct amounts. For this purpose, we benefitted from the results of our previous study[26] as the starting point. In our calculations, we

DOI: 10.1021/acsami.5b08377
ACS Appl. Mater. Interfaces 2015, 7, 23364−23371

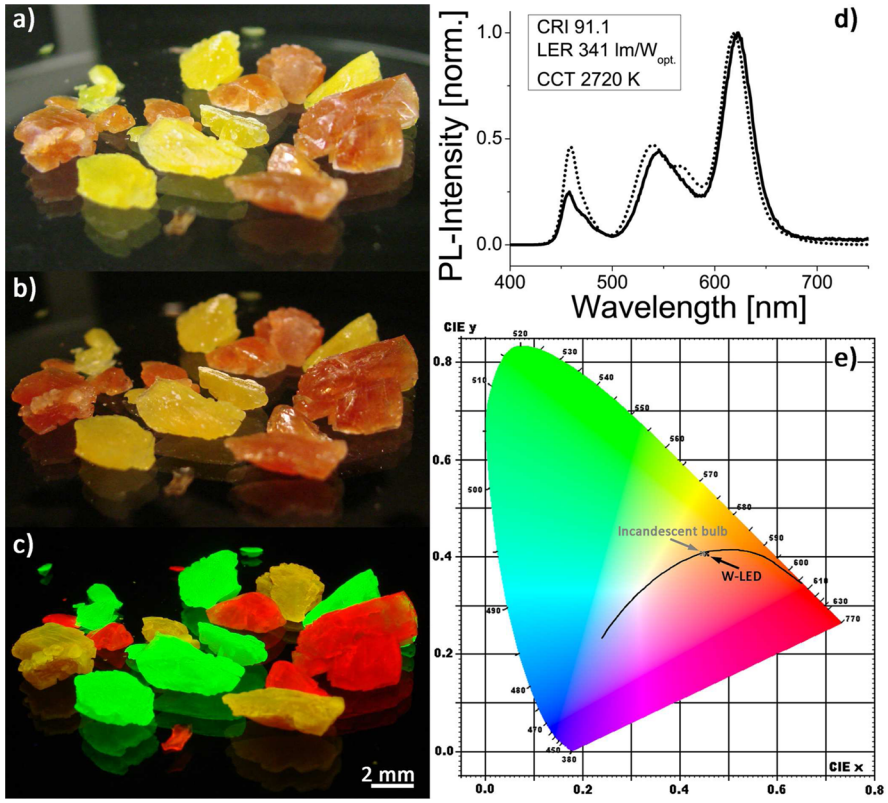

Figure 8. Photographs in panels a, b, and c show true color images of our mixed crystals under either ambient illumination with a standard fluorescence lamp (a), with our w-LED (b) and under 365 nm UV-excitation. Panel d presents the PL-spectra of our w-LED within the visible region (solid line) and the used modeled spectra (dotted line), whereas panel e shows a CIE 1931 diagram with the blackbody radiator (black line, CRI 100) as comparison, our w-LED marked with the black cross and an incandescent bulb (gray cross).

modeled the emission of the QDs as a Gaussian function unless we did not use the experimentally measured photoluminescence spectra. In our designs, we maximized the CRI, which indicates how well the real colors of the objects are rendered, and LER, which indicates how well the spectrum of the light source overlaps with the eye sensitivity curve. Furthermore, a special emphasis was given to generate a white light with a warm-white shade acquiring a CCT below 4500 K. According to our previous results, only a tiny fraction of all possible color combinations yields LED-spectra where CRI > 90, LER > 330 lm/W_{opt}, and CCT < 4500 K are obtained simultaneously. On the basis of these results, here we designed a four-color white LED composed of a blue LED chip pumping green, yellow, and red QD mixed crystals to generate white light. According to the recommendations provided at this step, we first synthesized green- and red-emitting QDs and grew their mixed crystals. Considering the measured photoluminescence spectra of these mixed crystals, the required peak emission wavelength of the yellow color component was determined to achieve CRI > 90, LER > 330 lm/W_{opt}, and CCT < 4500 K. On the basis of these results, we synthesized yellow QDs and grew their mixed crystals. Using the measured photoluminescence spectra of the green-, yellow-, and red-emitting mixed crystals, we calculated their necessary relative amplitudes for high-quality white light generation.

Chemicals and Apparatus. All chemicals used were of analytical grade or of the highest purity available. All aqueous solutions were prepared from Milli-Q water (Millipore).

Synthesis of QDs. CdSe/ZnS QDs with an alloyed gradient shell were synthesized according to a previous publication,[40] using slight modifications of the synthetic protocol. All amounts used for the synthesis can be found in Table S1.

For green (530 nm) and yellow (570 nm) emitting QDs, defined amounts of CdO, $Zn(OAc)_2$, oleic acid (OA), and 1-octadecene (ODE) were placed in a 50 mL three-necked flask. The mixture was degassed for 1 h and back-filled with inert gas at 100 °C. After the solution was heated to 310 °C, defined amounts of S and Se dissolved together in trioctylphosphine (TOP) were rapidly injected into the flask accompanied by a temperature reduction to 300 °C. After 10 min, the QD solution was cooled to room temperature, quenched with 20 mL of $CHCl_3$, and followed by two washing steps with an excess of acetone.

For red (617 nm)-emitting QDs, CdO, $Zn(OAc)_2$, OA, and ODE were placed in a 50 mL three-necked flask and the solution was degassed for 1 h at 100 °C. After the flask was back-filled with inert gas and heated to 300 °C, Se dissolved in TOP and ODE was injected rapidly into the flask, followed by a dropwise addition of 1-dodecanethiol (DDT) after 30 s. 20 min later, S dissolved in TOP was added dropwise to the reaction solution, while holding the mixture at 300 °C for a further 10 min. The QD solution was cooled to room temperature, quenched with 20 mL of $CHCl_3$, and washed two times with acetone and *i*-propanol. Finally, the QDs were redispersed in 4 mL of $CHCl_3$ to gain a concentrated solution for the ligand exchange and characterization.

Ligand Exchange. Long chain aliphatic acids on the QDs surface were exchanged with short chain thiols using a modified protocol from ref 28. 30 μL of concentrated QDs solution was diluted with 500 μL of $CHCl_3$ and mixed with a 0.2 M aqueous mercaptopropionic acid (MPA) solution at pH of 10. After the mixture was shaken vigorously for 4 h, the phases were separated, and the aqueous phase was used without further purification.

Preparation of QD−Salt Mixed Crystals. 2 mL of freshly ligand exchanged QD solution was mixed with 10 mL of saturated disodium tetraborate decahydrate $Na_2B_4O_7{\cdot}10H_2O$ (borax) solution, modifying our previous report.[19] The mixture was stored at 30 °C in an oven for about one week, until the parental solution turned colorless. The resulting mixed crystals were rinsed with cold water for cleaning, dried and stored under ambient conditions.

w-LED Preparation. To prepare white-emitting LEDs, the borax-based mixed crystals were milled to a fine powder and varying amounts of the differently emitting powders were blended with a two

DOI: 10.1021/acsami.5b08377
ACS Appl. Mater. Interfaces 2015, 7, 23364−23371

component silicone resin (ACC Silicones) on top of a blue-emitting commercial InGaN LED. The mixture was hardened for 2 h at 70 °C, forming a homogeneous color-conversion layer.

Preparation of Thin Sheets for Transmission Electron Microscopy (TEM). Structural characterization of QD−salt mixed crystals was performed using TEM. Prior to imaging, green-emitting and red-emitting mixed crystals were embedded into histological resin (Kulzer), which was prepared by mixing resin and cross-linker with a ratio of 15:1. To initiate the cross-linking process, samples were exposed to UV light at 254 nm for 15 min and then stored at room temperature for complete solidification. After 1 week, sheets of 200 nm thickness were obtained using a Leica ultramicrotome. Cross sections were transferred onto a Lacey carbon coated 200 mesh copper grid and TEM images were recorded using a FEI Tecnai G2 F30 transmission electron microscope.

Characterization. UV−vis absorption measurements were performed on a Cary 50 spectrophotometer (Varian). PL-spectra were recorded using a FluoroMax-4 spectrofluorometer (Horiba Jobin Yvon) at room temperature. PL-QY measurements of as-prepared and ligand exchanged QDs were performed according to ref 41 using Rhodamine 6G and Rhodamine 101 (both Radiant Dyes Laser) in ethanol (Uvasol, Merck), assuming their PL-QY as 91% and 91.5%, respectively, as luminescent standards.[41] Photoluminescence lifetime (PL-LT) traces were recorded using a Fluorolog-3 spectrofluorometer (Horiba Jobin Yvon) equipped with a pulsed LED diode and a time-correlated single-photon counting (TCSPC) module at room temperature. Average PL-LTs were calculated at the point in time where the initial signal intensity was reduced to 1/e. Absolute PL-QY measurements were performed using a FluoroLog-3 spectrofluorometer (Horiba Jobin Yvon) equipped with a Quanta-φ integrating sphere. Thermogravimetric analyses were performed on a TGA/DSC1 STAR^E System (Mettler-Toledo) using alumina crucibles and pressured air as purging gas. Anodic stripping voltammetric (ASV) analyses were performed on a PGSTAT 128N electrochemical workstation (Metrohm). The measurements were conducted in standard three-electrode configuration using a glassy carbon as the working electrode, a saturated calomel electrode (SCE) as the reference electrode, and a Pt-flag as the counter electrode. A detailed description of the measurement procedure is described in the literature.[42,43] The analyte concentration was determined by applying the standard addition method using a Cd standard solution.

Emission Stability Tests. We tested the stability of the mixed crystal emission by integrating green, yellow, and red mixed crystals on a blue LED. The LED was driven at 300 mA for 4 days. We recorded the emission intensity of the LEDs using a FluoroMax-4 spectrofluorometer (Horiba Jobin Yvon).

Temperature Tests. We measured the temperature of the LED chips using an FLIR A655sc infrared camera. The LEDs were operated by application of a square wave modulation (1 kHz, 50% duty cycle, 300 mA peak-to-peak current).

■ ASSOCIATED CONTENT

Supporting Information

The Supporting Information is available free of charge on the ACS Publications website at DOI: 10.1021/acsami.5b08377.

Synthetic parameters; PL-spectra of ligand exchanged CdSe/ZnS QDs as well as mixed crystals embedded into silicone films; true color images of NaCl and borax based mixed crystals; results of the anodic stripping voltammetric measurements; PL-LT traces; LED-temperature profiles as well as the thermogravimetric analyses data (PDF).

■ AUTHOR INFORMATION

Corresponding Authors

*N. Gaponik. E-mail: nikolai.gaponik@chemie.tu-dresden.de.
*H. V. Demir. E-mail: volkan@stanfordalumni.org.

Author Contributions

$^{\perp}$These authors contributed equally. The paper was written through contributions of all authors. All authors have given approval to the final version of the paper.

Notes

The authors declare no competing financial interest.

■ ACKNOWLEDGMENTS

All authors gratefully acknowledge the financial support from the EU-FP7 Network of Excellence Nanophotonics for Energy Efficiency (N4E) as well as from the BMBF TUR 09/001 and TUBITAK 112E183. T.E., Z.S.-E., and H.V.D. also acknowledge the financial support from TUBITAK EEEAG 109E002, 109E004, 110E010, 110E217, and 114F326 and from NRF-RF-2009-09, NRF-CRP-6-2010-02, and A*STAR of Singapore. H.V.D. also acknowledges generous support from ESF-EURYI and TUBA-GEBIP. T.E. additionally acknowledges the support of TUBITAK BIDEB.

■ REFERENCES

(1) UNESCO; DPG. Jahr des Lichtes. http://www.jahr-des-lichts.de/.

(2) UNESCO. The International Year of Light.http://www.unesco.org/new/en/unesco/events/prizes-and-celebrations/celebrations/international-years/international-year-of-light/ (accessed September 17, 2015).

(3) International Energy Agency. Energy efficiency: Lighting. http://www.iea.org/topics/energyefficiency/lighting/ (accessed September 17, 2015).

(4) *VERORDNUNG (EG) Nr. 244/2009*; European Union, 2009.

(5) Nakamura, S.; Senoh, M.; Mukai, T. High-Power InGaN/GaN Double-Heterostructure Violet Light Emitting Diodes. *Appl. Phys. Lett.* **1993**, *62* (19), 2390−2392.

(6) Mueller-Mach, R.; Mueller, G. O.; Krames, M. R.; Trottier, T. High-Power Phosphor-Converted Light-Emitting Diodes Based on III-Nitrides. *IEEE J. Sel. Top. Quantum Electron.* **2002**, *8* (2), 339−345.

(7) Krames, M. R.; Shchekin, O. B.; Mueller-Mach, R.; Mueller, G. O.; Zhou, L.; Harbers, G.; Craford, M. G. Status and Future of High-Power Light-Emitting Diodes for Solid-State Lighting. *J. Disp. Technol.* **2007**, *3* (2), 160−175.

(8) Ekimov, A. I.; Onushchenko, A. A. Quantum Size Effect in the Optical-Spectra of Semiconductor Micro-Crystals. *Semiconductors* **1982**, *16* (7), 775−778.

(9) Henglein, A. Photo-Degradation and Fluorescence of Colloidal-Cadmium Sulfide in Aqueous Solution. *Berichte der Bunsengesellschaft für Phys. Chemie* **1982**, *86* (4), 301−305.

(10) Brus, L. E. Electron−electron and Electron-Hole Interactions in Small Semiconductor Crystallites: The Size Dependence of the Lowest Excited Electronic State. *J. Chem. Phys.* **1984**, *80* (9), 4403−4409.

(11) Gaponik, N.; Hickey, S. G.; Dorfs, D.; Rogach, A. L.; Eychmüller, A. Progress in the Light Emission of Colloidal Semiconductor Nanocrystals. *Small* **2010**, *6* (13), 1364−1378.

(12) Achermann, M.; Petruska, M. A.; Koleske, D. D.; Crawford, M. H.; Klimov, V. I. Nanocrystal-Based Light-Emitting Diodes Utilizing High-Efficiency Nonradiative Energy Transfer for Color Conversion. *Nano Lett.* **2006**, *6* (7), 1396−1400.

(13) Demir, H. V.; Nizamoglu, S.; Erdem, T.; Mutlugun, E.; Gaponik, N.; Eychmüller, A. Quantum Dot Integrated LEDs Using Photonic and Excitonic Color Conversion. *Nano Today* **2011**, *6* (6), 632−647.

(14) Erdem, T.; Demir, H. V. Color Science of Nanocrystal Quantum Dots for Lighting and Displays. *Nanophotonics* **2013**, *2* (1), 57−81.

(15) Sun, C.; Zhang, Y.; Wang, Y.; Liu, W.; Kalytchuk, S.; Kershaw, S. V.; Zhang, T.; Zhang, X.; Zhao, J.; Yu, W. W.; Rogach, A. L. High Color Rendering Index White Light Emitting Diodes Fabricated from a Combination of Carbon Dots and Zinc Copper Indium Sulfide Quantum Dots. *Appl. Phys. Lett.* **2014**, *104* (26), 261106−4.

(16) QD Vision. http://www.qdvision.com/.

DOI: 10.1021/acsami.5b08377
ACS Appl. Mater. Interfaces 2015, 7, 23364−23371

(17) Lee, J.; Sundar, V. C.; Heine, J. R.; Bawendi, M. G.; Jensen, K. F. Full Color Emission from II-VI Semiconductor Quantum Dot-Polymer Composites. *Adv. Mater.* **2000**, *12* (15), 1102−1105.
(18) Otto, T.; Müller, M.; Mundra, P.; Lesnyak, V.; Demir, H. V.; Gaponik, N.; Eychmüller, A. Colloidal Nanocrystals Embedded in Macrocrystals: Robustness, Photostability, and Color Purity. *Nano Lett.* **2012**, *12* (10), 5348−5354.
(19) Müller, M.; Kaiser, M.; Stachowski, G. M.; Resch-Genger, U.; Gaponik, N.; Eychmüller, A. Photoluminescence Quantum Yield and Matrix-Induced Luminescence Enhancement of Colloidal Quantum Dots Embedded in Ionic Crystals. *Chem. Mater.* **2014**, *26* (10), 3231−3237.
(20) Kalytchuk, S.; Zhovtiuk, O.; Rogach, A. L. Sodium Chloride Protected CdTe Quantum Dot Based Solid-State Luminophores with High Color Quality and Fluorescence Efficiency. *Appl. Phys. Lett.* **2013**, *103* (10), 103105−4.
(21) Kim, T. H.; Wang, F.; McCormick, P.; Wang, L.; Brown, C.; Li, Q. Salt-Embedded Carbon Nanodots as a UV and Thermal Stable Fluorophore for Light-Emitting Diodes. *J. Lumin.* **2014**, *154*, 1−7.
(22) Erdem, T.; Soran-Erdem, Z.; Hernandez-Martinez, P. L.; Sharma, V. K.; Akcali, H.; Akcali, I.; Gaponik, N.; Eychmüller, A.; Demir, H. V. Sweet Plasmonics: Sucrose Macrocrystals of Metal Nanoparticles. *Nano Res.* **2015**, *8* (3), 860−869.
(23) Adam, M.; Tietze, R.; Gaponik, N.; Eychmüller, A. QD-Salt Mixed Crystals: The Influence of Salt-Type, Free-Stabilizer, and pH. *Z. Phys. Chem.* **2015**, *229* (1−2), 109−118.
(24) Adam, M.; Wang, Z.; Dubavik, A.; Stachowski, G. M.; Meerbach, C.; Soran-Erdem, Z.; Rengers, C.; Demir, H. V.; Gaponik, N.; Eychmüller, A. Liquid-Liquid Diffusion-Assisted Crystallization: A Fast and Versatile Approach Toward High Quality Mixed Quantum Dot-Salt Crystals. *Adv. Funct. Mater.* **2015**, *25* (18), 2638−2645.
(25) Phillips, J. M.; Coltrin, M. E.; Crawford, M. H.; Fischer, A. J.; Krames, M. R.; Mueller-Mach, R.; Mueller, G. O.; Ohno, Y.; Rohwer, L. E. S.; Simmons, J. A.; Tsao, J. Y. Research Challenges to Ultra-Efficient Inorganic Solid-State Lighting. *Laser Photonics Rev.* **2007**, *1* (4), 307−333.
(26) Erdem, T.; Nizamoglu, S.; Sun, X. W.; Demir, H. V. A Photometric Investigation of Ultra-Efficient LEDs with High Color Rendering Index and High Luminous Efficacy Employing Nanocrystal Quantum Dot Luminophores. *Opt. Express* **2010**, *18* (1), 340−347.
(27) *Commission Delegated Directive Amending, for the Purposes of Adapting to Technical Progress, Annex III to Directive 2011/65/EU of the European Parliament and of the Council as Regards an Exemption for Cadmium in Illumination and Display Lighting*; European Union, 2014.
(28) Tamang, S.; Beaune, G.; Texier, I.; Reiss, P. Aqueous Phase Transfer of InP/ZnS Nanocrystals Conserving Fluorescence and High Colloidal Stability. *ACS Nano* **2011**, *5* (12), 9392−9402.
(29) Breus, V. V.; Heyes, C. D.; Nienhaus, G. U. Quenching of CdSe−ZnS Core−Shell Quantum Dot Luminescence by Water-Soluble Thiolated Ligands. *J. Phys. Chem. C* **2007**, *111* (50), 18589−18594.
(30) Chang, Y.; Yao, X.; Mi, L.; Li, G.; Wang, S.; Wang, H.; Zhang, Z.; Jiang, Y. A Water−Ethanol Phase Assisted Co-Precipitation Approach toward High Quality Quantum Dot−Inorganic Salt Composites and Their Application for WLEDs. *Green Chem.* **2015**, *17* (8), 4439−4445.
(31) Chang, Y.; Yao, X.; Zhang, Z.; Jiang, D.; Yu, Y.; Mi, L.; Wang, H.; Li, G.; Yu, D.; Jiang, Y. Preparation of Highly Luminescent $BaSO_4$ Protected CdTe Quantum Dots as Conversion Materials for Excellent Color-Rendering White LEDs. *J. Mater. Chem. C* **2015**, *3* (12), 2831−2836.
(32) *Handbook of Chemistry and Physics*, 89th ed.; Lide, D. R., Ed.; Taylor & Francis Group: Boca Raton, FL, 2008.
(33) Wadhavane, P. D.; Galian, R. E.; Izquierdo, M. A.; Aguilera-Sigalat, J.; Galindo, F.; Schmidt, L.; Burguete, M. I.; Pérez-Prieto, J.; Luis, S. V. Photoluminescence Enhancement of CdSe Quantum Dots: A Case of Organogel−Nanoparticle Symbiosis. *J. Am. Chem. Soc.* **2012**, *134* (50), 20554−20563.
(34) Lakowicz, J. R. *Principles of Fluorescence Spectroscopy*, 3rd ed.; Springer-Verlag: New York, 2009.
(35) American National Standard for Electric Lamps − Specifications for the Chromaticity of Solid State Lighting Products; American National Standards Institute: Washington, DC, 2011.
(36) Nizamoglu, S.; Erdem, T.; Wei Sun, X.; Volkan Demir, H. Warm-White Light-Emitting Diodes Integrated with Colloidal Quantum Dots for High Luminous Efficacy and Color Rendering: Reply to Comment. *Opt. Lett.* **2011**, *36* (15), 2852.
(37) Wang, X.; Li, W.; Sun, K. Stable Efficient CdSe/CdS/ZnS Core/Multi-Shell Nanophosphors Fabricated through a Phosphine-Free Route for White Light-Emitting-Diodes with High Color Rendering Properties. *J. Mater. Chem.* **2011**, *21* (24), 8558−8565.
(38) Yuan, X.; Ma, R.; Zhang, W.; Hua, J.; Meng, X.; Zhong, X.; Zhang, J.; Zhao, J.; Li, H. Dual Emissive Manganese and Copper Co-Doped Zn−In−S Quantum Dots as a Single Color-Converter for High Color Rendering White-Light-Emitting Diodes. *ACS Appl. Mater. Interfaces* **2015**, *7* (16), 8659−8666.
(39) Zhang, Z.; Liu, D.; Li, D.; Huang, K.; Zhang, Y.; Shi, Z.; Xie, R.; Han, M.-Y.; Wang, Y.; Yang, W. Dual Emissive Cu:InP/ZnS/InP/ZnS Nanocrystals: Single-Source "Greener" Emitters with Flexibly Tunable Emission from Visible to Near-Infrared and Their Application in White Light-Emitting Diodes. *Chem. Mater.* **2015**, *27* (4), 1405−1411.
(40) Bae, W. K.; Kwak, J.; Lim, J.; Lee, D.; Nam, M. K.; Char, K.; Lee, C.; Lee, S. Multicolored Light-Emitting Diodes Based on All-Quantum-Dot Multilayer Films Using Layer-by-Layer Assembly Method. *Nano Lett.* **2010**, *10* (7), 2368−2373.
(41) Würth, C.; Grabolle, M.; Pauli, J.; Spieles, M.; Resch-Genger, U. Relative and Absolute Determination of Fluorescence Quantum Yields of Transparent Samples. *Nat. Protoc.* **2013**, *8* (8), 1535−1550.
(42) Wang, J. Stripping Analysis at Bismuth Electrodes: A Review. *Electroanalysis* **2005**, *17* (15−16), 1341−1346.
(43) Prior, C.; Walker, G. S. The Use of the Bismuth Film Electrode for the Anodic Stripping Voltammetric Determination of Tin. *Electroanalysis* **2006**, *18* (8), 823−829.

DOI: 10.1021/acsami.5b08377
ACS Appl. Mater. Interfaces 2015, 7, 23364−23371